NONLINEAR EDGE EFFECT ANALYSIS OF LAMINATED BEAMS WITH PIEZOELECTRIC LAYERS

Masoud Tahani[1,2] and Mojtaba Izadi[1]

[1] Department of Mechanical Engineering, Faculty of Engineering, Ferdowsi University of Mashhad, Mashhad, Iran
[2] Iranian Academic Center for Education, Culture and Research (ACECR), Mashhad Branch, Iran.
mtahani@ferdowsi.um.ac.ir

ABSTRACT

An analytical solution is presented to determine the interlaminar stresses of general cross-ply laminated beams with piezoelectric layers. The displacement field is assumed within the framework of a third-order shear deformation beam theory. The strain components are obtaind using von-Kàrmàn nonlinear strain-displacement relations. Also, it is assumed that the electric potential varies linearly through the thickness of each layer. Using the principle of minimum total potential energy, equilibrium equations are obtained in terms of stress resultants. Finally, a set of ordinary differential equations with constant coefficients are obtained. The solutions of the equations are the unknown assumed functions for displacement field. Numerical results clearly indicate the singular behavior of interlaminar normal and shear stresses near the ends of the laminated beam.

1. INTRODUCTION

Composite materials produce properties that cannot be achieved by their constituents alone. Some of the properties are stiffness, weight reduction, corrosion resistance, thermal properties, fatigue life, and wear resistance. These properties made the use of composites increasing steadily.

The use of sensors and actuators to perform a self-controlling and self-monitoring system has produced a new class of structures known as “smart structures”. Smart structures incorporating piezoelectric devices to sense and actuate the structure could be applied in many advanced engineering applications, such as aircraft structures, satellites, large space structures and so forth [1]. A great enhancement to smart structures has been given by advanced fiber reinforced composites. Laminated composites are very well suited to include a network of piezoelectric sensors and actuators and then form a smart structure. To advance this technology further and apply it to complex and realistic products, a thorough and comprehensive knowledge of piezoelectric composites is necessary.

Also, there are some problems which need to be overcome before piezoelectric composites can be widely used. Among the problems, delamination has received very much attention due to its significant effect on strength and stiffness. Delamination is caused by high interlaminar stresses on the interface of composite layers. Certain interlaminar stress components exhibit a mathematical singular behavior at the edges of a laminated structure. This effect is commonly called the edge effect, the investigation of which has prefaced by the pioneering work of Pipes and Pagano [2] who employed a finite differences technique. To date many analytical and numerical approaches have been developed and applied. A comprehensive discussion of the literature on the interlaminar stress problem in composite laminates is given in [3].

However, there are not much many studies including the edge effect of piezoelectric composite laminated structures. The coupled piezoelectric analysis of the free edge effect has been performed by Davi and Milazzo [4], who investigated a $[\pm 45°]_s$ laminate

under several loading conditions using boundary element formulation. In that work, no significant influence of piezoelectric coupling on the interlaminar stresses could be detected. Artel and Becker [5] analyzed the influence of piezoelectric coupling on interlaminar stresses and electric field near the edge, using the finite element method. They showed that for the cross-ply laminates under consideration, some interlaminar stress components near the edge become singular and in the coupled analysis case are usually of higher magnitude than in the uncoupled analysis. Erturk and Tekinalp [6] and also Zhen and Wanji [7] introduced new types of elements, for finite element approach, and analyzed the interlaminar stresses of piezoelectric composite laminated beams and plates. Finally, the study of the interlayer stresses and their concentrations near the two ends of a laminated beam of piezoelectric and elastic material has been performed by Yang et. al. [8] using 3D finite element method. They addressed the influence of geometrical and material parameters on the edge effect.
As it is seen, yet there are no analytical investigations including the edge effect in composite laminated structures with piezoelectric layers. In this paper an analytical solution is obtained to determine the nonlinear interlaminar stresses of a general cross-ply composite laminated beam, which has piezoelectric layers.

2. MATHEMATICAL FORMULATION

It is intended here to determine the interlaminar stresses in a cross-ply laminated beam with dimensions l and h as its length and height, as shown in Figure 1. Some of the layers have piezoelectric properties and it is assumed that the electrodes for applying voltage are placed at the layer interfaces. The displacement field using a third-order shear deformation beam theory (TSDBT) may be represented as:

$$\begin{aligned} u_1(x,y,z) &= u_0(x) + z\psi_x(x) + z^2\varphi_x(x) + z^3\eta_x(x), \\ u_2(x,y,z) &= 0, \\ u_3(x,y,z) &= w(x) + z\psi_z(x). \end{aligned} \tag{1}$$

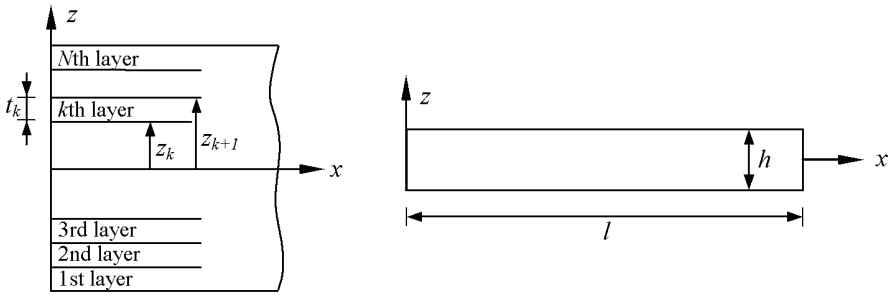

Figure 1: Geometry of the piezoelectric laminated beam.

where u_1, u_2, and u_3 are displacements in the x, y, and z directions, respectively, of a material point initially located at (x, y, z) in the undeformed beam. As the beam is formed of cross-ply layers, no displacement in y direction will occur. Substituting Equations (1) into the von-Kàrmàn nonlinear strain-displacement relations, the following results will be obtained [9]:

$$\begin{aligned} &\varepsilon_x = u_0' + (w')^2/2 + z\psi_x', + z^2\varphi_x' + z^3\eta_x', \quad \varepsilon_z = \psi_z, \\ &\gamma_{xz} = \psi_x + w' + z(2\varphi_x + \psi_z') + 3z^2\eta_x, \quad \varepsilon_y = \gamma_{yz} = \gamma_{xy} = 0. \end{aligned} \tag{2}$$

A prime in these equations indicates an ordinary derivative with respect to x. Using the principle of minimum total potential energy, equilibrium equations can be obtained in

terms of stress resultants as [9]:

$$\begin{aligned} &\frac{\mathrm{d}N_x}{\mathrm{d}x}=0, \qquad \frac{\mathrm{d}M_x}{\mathrm{d}x}-Q_x=0, \qquad \frac{\mathrm{d}L_x}{\mathrm{d}x}-2R_x=0,\\ &\frac{\mathrm{d}P_x}{\mathrm{d}x}-3S_x=0, \qquad \frac{\mathrm{d}}{\mathrm{d}x}(N_x w'+Q_x)=0, \qquad \frac{\mathrm{d}R_x}{\mathrm{d}x}-N_z=0. \end{aligned} \tag{3}$$

The stress resultants in Equations (3) are defined as:

$$\begin{aligned} &(N_x, M_x, L_x, P_x)=\int_{-h/2}^{h/2}(1, z, z^2, z^3)\sigma_x \mathrm{d}z,\\ &N_z=\int_{-h/2}^{h/2}\sigma_z \mathrm{d}z, \quad (Q_x, R_x, S_x)=\int_{-h/2}^{h/2}(1, z, z^2)\sigma_{xz}\mathrm{d}z. \end{aligned} \tag{4}$$

Three types of boundary conditions can be defined at the ends of the beam, given in Table 1.

Table 1: Types of boundary conditions at the ends of the beam

Type	Symbol	Conditions
Simple support	S1	$N_x=M_x=L_x=P_x=w=R_x=0$
	S2	$u_0=M_x=L_x=P_x=w=R_x=0$
Clamped	C	$u_0=\psi_x=\varphi_x=\eta_x=w=\psi_z=0$
Free	F	$N_x=M_x=L_x=P_x=Q_x=R_x=0$

3. GVERNING EQUATIONS OF EQUILIBRIUM

Because the width of the beam is small comparing to its length, it is assumed that $\sigma_y = \sigma_{yz} = 0$ [10], so the reduced piezo-elastic constitutive law of the *k*th orthotropic piezoelectric lamina with fiber orientations of 0º or 90º only is utilized as [11]:

$$\begin{Bmatrix}\sigma_x\\ \sigma_z\\ \sigma_{xy}\\ \sigma_{xz}\end{Bmatrix}^{(k)}=\begin{bmatrix}\bar{\bar{C}}_{11} & \bar{\bar{C}}_{13} & 0 & 0\\ \bar{\bar{C}}_{13} & \bar{\bar{C}}_{33} & 0 & 0\\ 0 & 0 & \bar{\bar{C}}_{66} & 0\\ 0 & 0 & 0 & \bar{\bar{C}}_{55}\end{bmatrix}^{(k)}\begin{Bmatrix}\varepsilon_x\\ \varepsilon_z\\ \gamma_{xy}\\ \gamma_{xz}\end{Bmatrix}-\begin{bmatrix}\bar{\bar{e}}_{13}\\ \bar{\bar{e}}_{33}\\ 0\\ 0\end{bmatrix}^{(k)}\{E_z\}^{(k)}, \tag{5}$$

where $\{\sigma\}$ and $\{\varepsilon\}$ are the stress and strain vectors, $[\bar{\bar{C}}]^{(k)}$ and $[\bar{\bar{e}}]^{(k)}$ are the off-axis reduced mechanical stiffness and piezoelectric coupling matrices, given in Appendix, and $\{E\}^{(k)}$ is the electric field vector, whose components are defined as:

$$E_x^{(k)}=-\frac{\partial \phi_e^{(k)}}{\partial x}, \quad E_y^{(k)}=-\frac{\partial \phi_e^{(k)}}{\partial y}, \quad E_z^{(k)}=-\frac{\partial \phi_e^{(k)}}{\partial z}, \tag{6}$$

with $\phi_e^{(k)}(x, y, z)$ being the scalar function of electric potential through the *k*th layer. It should be noted that electric voltage is applied to piezoelectric layers through the thickness. It is assumed that the electric potential $\phi_e^{(k)}$ varies linearly in the *z*-direction through each layer [12-13], so $\phi_e^{(k)}(x, y, z)$ reduces to:

$$\phi_e^{(k)}(x, y, z)=\phi_e^{(k)}(z)=\frac{\phi_{e,z_{k+1}}-\phi_{e,z_k}}{t_k}, \tag{7}$$

where $\phi_{e,z_{k+1}}$ is the electric voltage applied at the upper interface and t_k is the thickness of the kth layer (see Figure 1). By this assumption, only the component E_z of the electric field exists which is a constant for each layer.

It is convenient to introduce a new unknown function which will let us to handle the nonlinear terms. This function is defined as:

$$\overline{u}'(x) = \varepsilon_1^0(x) = u_0' + (w')^2/2 \tag{8}$$

Upon substitution of Equations (2) and (8) into Equation (5) and the subsequent results into Equations (4), the generalized stress resultants are obtained, which can be represented as follows:

$$\begin{aligned}
N_x &= \overline{A}_{11}\overline{u}' + \overline{B}_{11}\psi_x' + \overline{D}_{11}\varphi_x' + \overline{E}_{11}\eta_x' + \overline{A}_{13}\psi_z - N_x^P,\\
M_x &= \overline{B}_{11}\overline{u}' + \overline{D}_{11}\psi_x' + \overline{E}_{11}\varphi_x' + \overline{F}_{11}\eta_x' + \overline{B}_{13}\psi_z - M_x^P,\\
L_x &= \overline{D}_{11}\overline{u}' + \overline{E}_{11}\psi_x' + \overline{F}_{11}\varphi_x + \overline{G}_{11}\eta_x' + \overline{D}_{13}\psi_z - L_x^P,\\
P_x &= \overline{E}_{11}\overline{u}' + \overline{F}_{11}\psi_x' + \overline{G}_{11}\varphi' + \overline{H}_{11}\eta_x' + \overline{E}_{13}\psi_z - P_x^P,\\
N_z &= \overline{A}_{13}\overline{u}' + \overline{B}_{13}\psi_x' + \overline{D}_{13}\varphi_x' + \overline{E}_{13}\eta_x' + \overline{A}_{33}\psi_z - N_z^P,\\
Q_x &= \overline{A}_{55}(\psi_x + w') + \overline{B}_{55}(2\varphi_x + \psi_z') + 3\overline{D}_{55}\eta_x,\\
R_x &= \overline{B}_{55}(\psi_x + w') + \overline{D}_{55}(2\varphi_x + \psi_z') + 3\overline{E}_{55}\eta_x,\\
S_x &= \overline{D}_{55}(\psi_x + w') + \overline{E}_{55}(2\varphi_x + \psi_z') + 3\overline{F}_{55}\eta_x.
\end{aligned} \tag{9}$$

The rigidity terms in Equations (9) are given by:

$$(\overline{A}_{ij}, \overline{B}_{ij}, \overline{D}_{ij}, \overline{E}_{ij}, \overline{F}_{ij}, \overline{G}_{ij}, \overline{H}_{ij}) = \sum_{k=1}^{N} \int_{z_k}^{z_{k+1}} (1, z, z^2, z^3, z^4, z^5, z^6)\overline{\overline{C}}_{ij}^{(k)}\mathrm{d}z. \tag{10}$$

Note that the integration of the electric terms in Equation (5) with respect to z are some constants, indicated by superscript P in Equations (9), defined as:

$$(N_x^P, M_x^P, L_x^P, P_x^P) = \int_{-h/2}^{h/2} (1, z, z^2, z^3)\overline{\overline{e}}_{13}^{(k)}E_z\mathrm{d}z, \quad N_z^P = \int_{-h/2}^{h/2} \overline{\overline{e}}_{33}^{(k)}E_z\mathrm{d}z. \tag{11}$$

To obtain the governing equations of equilibrium, first note that from the first equation of (3), we have:

$$N_x = N_x^0 \tag{12}$$

where N_x^0 is a constant to be found from boundary conditions. Substituting Equation (9) into (3) yields the governing equations of equilibrium, which is a set of ordinary differential equations whose characteristic equation has repeated zero roots. In order to enhance the solution scheme of these equations, some small artificial terms will be added to these equations so that the characteristic roots become all distinct [14-15]. Therefore, these equations are rewritten as follows:

$$\begin{aligned}
&\overline{A}_{11}\overline{u}'' + \alpha_1\overline{u} + \overline{B}_{11}\psi_x'' + \overline{D}_{11}\varphi_x'' + \overline{E}_{11}\eta_x'' + \overline{A}_{13}\psi_z' = 0,\\
&\overline{B}_{11}\overline{u}'' + \overline{D}_{11}\psi_x'' - \overline{A}_{55}\psi_x + \overline{E}_{11}\varphi_x'' - 2\overline{B}_{55}\varphi_x + \overline{F}_{11}\eta_x'' - 3\overline{D}_{55}\eta_x - \overline{A}_{55}w' + (\overline{B}_{13} - \overline{B}_{55})\psi_z' = 0,\\
&\overline{D}_{11}\overline{u}'' + \overline{E}_{11}\psi_x'' - 2\overline{B}_{55}\psi_x + \overline{F}_{11}\varphi_x'' - 4\overline{D}_{55}\varphi_x + \overline{G}_{11}\eta_x'' - 6\overline{E}_{55}\eta_x - 2\overline{B}_{55}w' + (\overline{D}_{13} - 2\overline{D}_{55})\psi_z' = 0,\\
&\overline{E}_{11}\overline{u}'' + \overline{F}_{11}\psi_x'' - 3\overline{D}_{55}\psi_x + \overline{G}_{11}\varphi_x'' - 6\overline{E}_{55}\varphi_x + \overline{H}_{11}\eta_x'' - 9\overline{F}_{55}\eta_x - 3\overline{D}_{55}w' + (\overline{E}_{13} - 3\overline{E}_{55})\psi_z' = 0,\\
&\overline{A}_{55}\psi_x' + 2\overline{B}_{55}\varphi_x' + 3\overline{D}_{55}\eta_x' + (\overline{A}_{55} + N_x^0)w'' + \alpha_2 w + \overline{B}_{55}\psi_z'' = 0,\\
&-\overline{A}_{13}\overline{u}' + (\overline{B}_{55} - \overline{B}_{13})\psi_x' + (2\overline{D}_{55} - \overline{D}_{13})\varphi_x' + \overline{B}_{55}w'' + (3\overline{E}_{55} - \overline{E}_{13})\eta_x' + \overline{D}_{55}\psi_z'' - \overline{A}_{33}\psi_z = -N_z^P.
\end{aligned} \tag{13}$$

with α_1 and α_2 being prescribed numbers which are relatively small compared to the numerical values of stiffnesses A_{ij}, B_{ij}, etc. This way the solution of the Equations (13) will extremely be insensitive to the small number chosen for the parameters α_1 and α_2. The solution of Equations (13) may be found by using state-space approach [16] as (see Appendix):

$$\begin{aligned} &\bar{u}(x)=\sum_{i=1}^{12}T_{1i}K_i e^{\lambda_i x}, \quad \psi_x(x)=\sum_{i=1}^{12}T_{3i}K_i e^{\lambda_i x}, \qquad \varphi_x(x)=\sum_{i=1}^{12}T_{5i}K_i e^{\lambda_i x}, \\ &\eta_x(x)=\sum_{i=1}^{12}T_{7i}K_i e^{\lambda_i x}, \quad w(x)=\sum_{i=1}^{12}T_{9i}K_i e^{\lambda_i x}, \quad \psi_z(x)=\sum_{i=1}^{12}T_{11i}K_i e^{\lambda_i x}+\frac{N_z^P}{\bar{A}_{33}}. \end{aligned} \tag{14}$$

Here, [T] and λ_i's (i = 1, 2, ... , 12) are, respectively, the matrix of eigenvectors and eigenvalues of the coefficient matrix of Equations (13) given in Appendix, which may have complex values. Also K_i's are twelve arbitrary unknown constants of integration to be found by imposing the boundary conditions at the ends of the beam.

It can be shown that if one of the boundary conditions at each end of the beam was N_x = 0, the nonlinear analysis would lead to same results as the linear one. So, only S2 and C type conditions are taken into consideration (see Table 1), for which u_0 = 0. Since the function $u_0(x)$ does not appear implicitly in Equations (14), this boundary condition can not be imposed directly. Instead, the condition given in Equation (12) at the both ends of the beam is used to find the unknown constants K_i's.

4. NUMERICAL RESULTS

A try and error procedure should be utilized, to obtain the solutions given in Equations (14). To this end, a numerical value is assigned to N_x^0. Then, Equation (8) is integrated with respect to x from 0 to l to get:

$$\bar{u}(l)-\bar{u}(0)=u_0(l)-u_0(0)+\int_0^l \frac{1}{2}(w')^2\,\mathrm{d}x. \tag{15}$$

This condition is used to modify the numerical value of N_x^0.

Equation (5) is used to find the in-plane stress σ_x. For interlaminar stresses σ_z and σ_{xz} local equilibrium equations are integrated to improve the accuracy [14-15]. Since the nonlinear strain-displacement relations are considered, local equilibrium equations should be stated in terms of Piola-Kirchoff stress tensor, which may take the following form for the beam:

$$\frac{\partial \sigma_{xy}}{\partial x}+\frac{\partial \sigma_{yz}}{\partial z}=0, \qquad \frac{\partial}{\partial x}\left(\sigma_x w'+\sigma_{xz}\right)+\frac{\partial}{\partial z}\left(\sigma_{xz} w'+\sigma_z\right)=0. \tag{16}$$

To test the reliability of the analysis, the methodology outlined previously is applied to a laminated beam, which is subjected to the S2-type of simply supported boundary conditions at x = 0,l. This case of simply supported beam is compared against corresponding numerical results based on a first-order shear deformation beam theory (FSDBT). The laminated beam with ply configuration $[0°/90°]_s$ is assumed to have the thickness h and length l and each of the material layers are of equal thickness $t_k = t = h/4$ (see Figure 1). The employed material is supposed to be idealized as a homogeneous piezoelectric orthotropic composite material with the mechanical properties of a typical high-modulus graphite/epoxy lamina [2] and electrical properties of PZT-5A [5] as follows:

E_1 = 137.9 GPa, $E_2 = E_3$ = 14.48 GPa, $G_{12} = G_{13} = G_{23}$ = 5.86 GPa,
$\upsilon_{12} = \upsilon_{13} = \upsilon_{23}$ = 0.21,

$e_{31} = e_{32} = -5.4$ C/m^2, $e_{33} = 15.8$ C/m^2, $e_{24} = e_{15} = 12.3$ C/m^2, (17)

where the subscripts 1, 2, and 3 indicate the principal material coordinates. The voltage $V_a = 200$ kV is applied to the upper layer of the beam. The beam geometry is mainly determined by $l = 10h$ and $h=0.01$ m.

Figure 2 shows the deflection of the beam in terms of its length. Also Figure 3 illustrates the distribution of in-plane stress σ_x through the thickness of the beam at $x = l/2$. Obviously, good agreement between third-order and first-order theories is found.

After the reliability of the method has successfully been tested, let's check the necessity of the nonlinear analysis. Maximum deflection of the same beam in terms of the applied voltage V_a is shown in Figure 4 for both linear and nonlinear analysis. As it is expected, as the magnitude of the applied voltage increased, the difference between linear and nonlinear analysis becomes considerable. This means that at high voltages, one should use the nonlinear analysis.

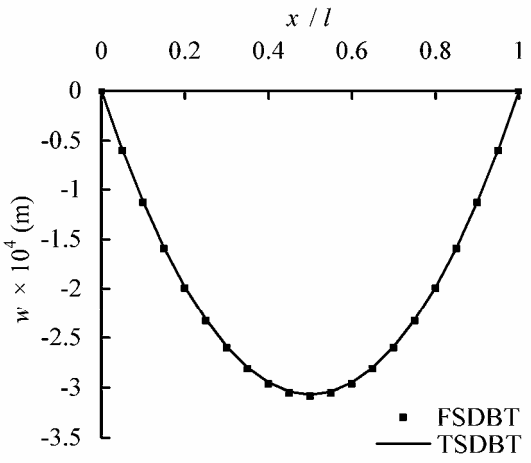

Figure 2: Deflection of a S2S2 $[0°/90°]_s$ beam.

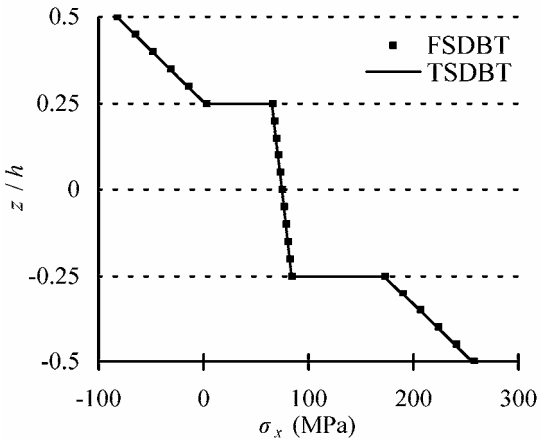

Figure 3: Distribution of in-plane stress σ_x through the thickness of the S2S2 $[0°/90°]_s$ beam at $x = l/2$.

Next, the behavior of interlaminar stresses of the same laminated beam is presented. Figure 5 shows the distributions of σ_z and σ_{xz} along the middle plane and 0°/90° interfaces of $[0°/90°]_s$ beam. The singular behavior of the interlaminar stresses is clearly observed in this figure.

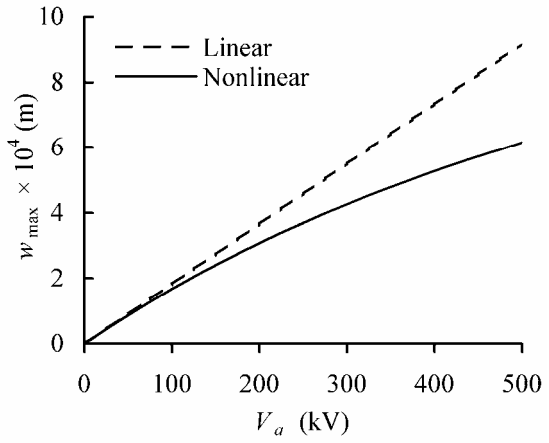

Figure 4: Maximum deflection of the S2S2 $[0°/90°]_s$ beam in terms of the applied voltage to the upper surface of the beam.

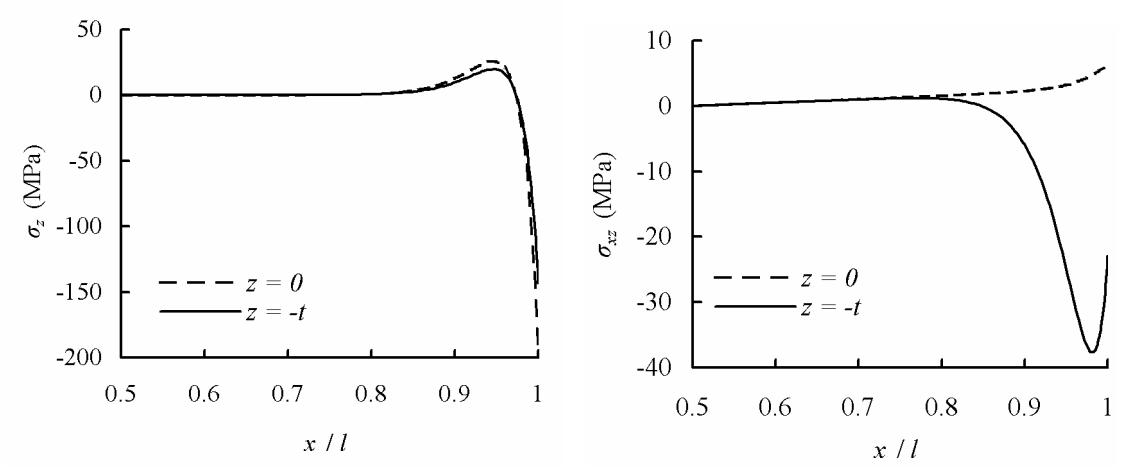

(a) (b)

Figure 5: Distributions of (a) interlaminar normal stress σ_z and (b) interlaminar shear stress σ_{xz} through the length of the S2S2 $[0°/90°]_s$ beam.

Figure 6 shows the distributions of interlaminar normal and shear stresses at all three layer interfaces of the asymmetric $[0°/90°]_2$ beam through the length. The boundary condition for this lay-up is S2-type at the both ends and the voltage $V_a = 200$ kV is applied to the upper surface.

The last example is presented to investigate the effect of beam's aspect ratio *l*/*h* on interlaminar stresses. To be able to compare different beams, the interlaminar stresses are nondimensionalized as:

$$(\bar{\sigma}_z, \bar{\sigma}_{xz}) = (\sigma_z, \sigma_{xz}) \frac{l}{e_{31} V_a} \tag{18}$$

where V_a is the voltage applied to the upper surface of the beam. Figure 7 shows the distributions of $\bar{\sigma}_z$ and $\bar{\sigma}_{xz}$ through the middle plane of S2S2 supported $[90°/0°]_s$ beams with different aspect ratios. It is seen as the thickness of the beam decreases, the magnitude of both interlaminar normal and shear stresses increase and their behavior becomes more singular.

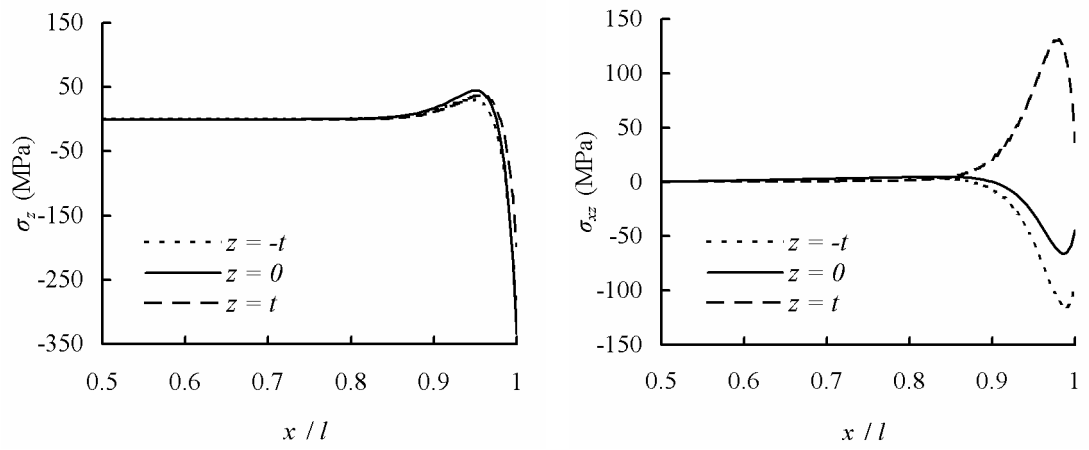

(a) (b)

Figure 6: Distributions of (a) interlaminar normal stress σ_z and (b) interlaminar shear stress σ_{xz} through the length of a S2S2 $[0°/90°]_2$ beam.

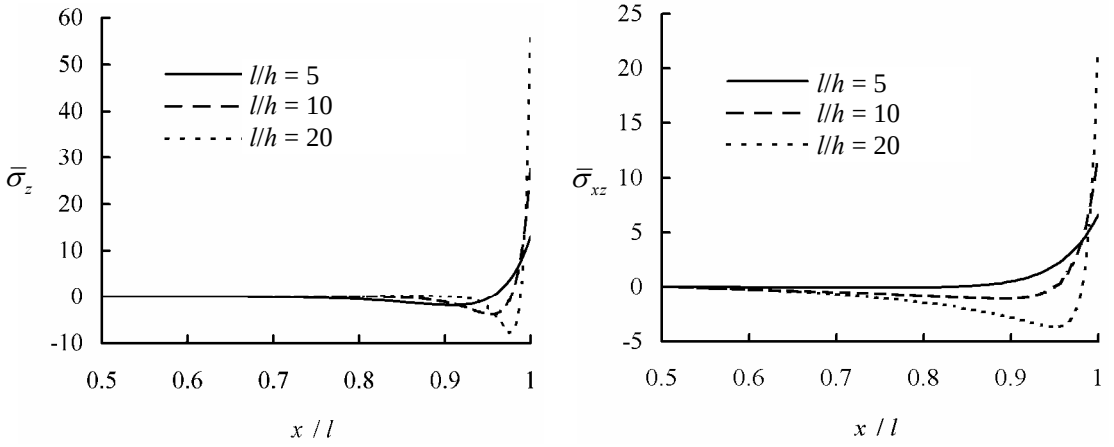

(a) (b)

Figure 7: Distributions of (a) interlaminar normal stress $\bar{\sigma}_z$ and (b) interlaminar shear stress $\bar{\sigma}_{xz}$ through the middle plane of the S2S2 $[90°/0°]_s$ beam for different aspect ratios.

5. CONCLUSIONS

An analytical solution has been performed to investigate the interlaminar stresses in general cross-ply composite laminated beams with piezoelectric layers. Equilibrium equations have been obtained within the framework of a third-order shear deformation beam theory. The solution can be used for different boundary conditions at the ends of the beams subjected to electrical loading. Also it is assumed that the electric potential varies linearly through the thickness of each layer. The singular behavior of the interlaminar stresses in the boundary-layer region for both symmetric and asymmetric lay-ups is obviously seen in the numerical results.

REFERENCES

1- Crawley, E.F. and de Luis, J., "Use of piezoelectric actuators as elements of intelligent structures", *AIAA Journal*, 1987; 25: 1373-1385.

2- Pipes, R.B. and Pagano, N.J., "Interlaminar stresses in composite laminates under uniform axial extension", *Journal of Composite Matererials*, 1970;4:538-548.

3- Kant, T. and Swaminathan, K., "Estimation of transversely interlaminar stresses in laminated composites—a selective review and survey of current developments", *Composite Structures*, 2000;49:65-75.
4- Davi, G. and Milazzo, A., "Stress and electric fields in piezoelectric composite laminates", *Electronic Journal of Boundary Elements*, 2002;Beteq 1:43-50.
5- Artel, J. and Becker, W., "Coupled and uncoupled analyses of piezoelectric free edge effect in laminated plates", *Composite Structures*, 2005;69:329-335.
6- Erturk, C.L. and Tekinalp, O., "A layerwise approach to piezoelectric plates accounting for adhesive flexibility and delaminated regions", *Computers and Structures*, 2005;83:279–296.
7- Zhen, W. and Wanji, C., "Refined triangular element for laminated elastic–piezoelectric plates", *Composite Structures*, 2007;78:129-139.
8- Yang, Q.S., Qin, Q.H., Liu, T., "Interlayer stress in laminate beam of piezoelectric and elastic materials", *Composite Structures*, 2006;75:587-592.
9- Reddy, J.N., *Energy principles and variational methods in applied mechanics*, 2002, John Wiley & Sons, Inc., New Jersey.
10- Tahani, M., "Analysis of laminated composite beams using layerwise displacement theories", *Composite Structures*, 2007;79:535-547.
11- Reddy, J.N., *Mechanics of laminated plates and shells*, 2003, 2nd Ed., CRC Press, Florida.
12- Franco Correia, V.M., Aguiar Gomes, M.A., Suleman, A., Mota Soares, C.M., Mota Soares, C.A., "Modeling and design of adaptive composite structures", *Computer Methods in Applied Mechanics and Engineering*, 2000;185:325-346.
13- Saravanos, D.A., "Mixed laminate theory and finite element for smart piezoelectric composite shell structures", *AIAA Journal*, 1997;35:1327-1333.
14- Tahani, M. and Nosier, A., "Free edge stress analysis of general cross-ply composite laminates under extension and thermal loading", *Composite Structures*, 2003;60:91-103.
15- Tahani, M. and Nosier, A., "Accurate determination of interlaminar stresses in general cress-ply laminates", *Mechanics of Advanced Materials and Structures*, 2004;11:67-92.
16- Gopal, M., *Modern Control System Theory*, 1993, 2nd Ed., New Age International (P) Limited.

APPENDIX

The general constitutive relation for the *k*th orthotropic piezoelectric material is given by:

$$\{\sigma\}^{(k)} = \left[\bar{C}\right]^{(k)} \{\varepsilon\}^{(k)} - \left[\bar{e}\right]^{(k)} \{E\}^{(k)}.$$

For beams, as it is mentioned, this relation is reduced to Equation (5) where the off-axis reduced mechanical stiffness and piezoelectric coupling matrices are defined as:

$$\begin{bmatrix} \bar{\bar{C}}_{11} & \bar{\bar{C}}_{13} & 0 \\ \bar{\bar{C}}_{13} & \bar{\bar{C}}_{33} & 0 \\ 0 & 0 & \bar{\bar{C}}_{66} \end{bmatrix}^{(k)} = \left(\begin{bmatrix} \bar{S}_{11} & \bar{S}_{13} & 0 \\ \bar{S}_{13} & \bar{S}_{33} & 0 \\ 0 & 0 & \bar{S}_{66} \end{bmatrix}^{(k)} \right)^{-1},$$

$$\begin{bmatrix} \bar{\bar{e}}_{13} \\ \bar{\bar{e}}_{33} \\ 0 \end{bmatrix} = \left(\begin{bmatrix} \bar{S}_{11} & \bar{S}_{13} & 0 \\ \bar{S}_{13} & \bar{S}_{33} & 0 \\ 0 & 0 & \bar{S}_{66} \end{bmatrix}^{-1} \begin{bmatrix} \bar{d}_{13} \\ \bar{d}_{33} \\ 0 \end{bmatrix} \right)^{(k)}, \quad \bar{\bar{C}}_{55}^{(k)} = 1/\bar{S}_{55}^{(k)}.$$

In order to solve Equations (13), the state-space variables are assumed as:

$$\xi_1 = \bar{u}, \quad \xi_2 = \bar{u}', \quad \xi_3 = \psi_x, \quad \xi_4 = \psi',$$
$$\xi_5 = \varphi_x, \quad \xi_6 = \varphi', \quad \xi_7 = \eta_x, \quad \xi_8 = \eta_x',$$
$$\xi_9 = w, \quad \xi_{10} = w', \quad \xi_{11} = \psi_z, \quad \xi_{12} = \psi_z'.$$

Substitution of these variables into Equations (13) results in a system of twelve coupled first-order ordinary differential equations, which may be presented as $\{\xi'\} = [A]\{\xi\}$ where $\{\xi\} = \left[\xi_1, \xi_2, ..., \xi_{12}\right]^T$ and $[A] = [Q]^{-1}[R]$ with

$$[Q] = \begin{bmatrix} 1 & 0 & 0 & 0 & 0 & 0 & 0 & 0 & 0 & 0 & 0 & 0 \\ 0 & A_{11} & 0 & B_{11} & 0 & D_{11} & 0 & E_{11} & 0 & 0 & 0 & 0 \\ 0 & 0 & 1 & 0 & 0 & 0 & 0 & 0 & 0 & 0 & 0 & 0 \\ 0 & B_{11} & 0 & D_{11} & 0 & E_{11} & 0 & F_{11} & 0 & 0 & 0 & 0 \\ 0 & 0 & 0 & 0 & 1 & 0 & 0 & 0 & 0 & 0 & 0 & 0 \\ 0 & D_{11} & 0 & E_{11} & 0 & F_{11} & 0 & G_{11} & 0 & 0 & 0 & 0 \\ 0 & 0 & 0 & 0 & 0 & 0 & 1 & 0 & 0 & 0 & 0 & 0 \\ 0 & E_{11} & 0 & F_{11} & 0 & G_{11} & 0 & H_{11} & 0 & 0 & 0 & 0 \\ 0 & 0 & 0 & 0 & 0 & 0 & 0 & 0 & 1 & 0 & 0 & 0 \\ 0 & 0 & 0 & 0 & 0 & 0 & 0 & 0 & 0 & A_{55} + N_x^0 & 0 & B_{55} \\ 0 & 0 & 0 & 0 & 0 & 0 & 0 & 0 & 0 & 0 & 1 & 0 \\ 0 & 0 & 0 & 0 & 0 & 0 & 0 & 0 & 0 & B_{55} & 0 & D_{55} \end{bmatrix}$$

and [R] is a 12×12 matrix whose nonzero elements are:

$$R_{1,2} = 1, \quad R_{2,1} = -\alpha_1, \quad R_{2,12} = -A_{13}, \quad R_{3,4} = 1,$$
$$R_{4,3} = A_{55}, \quad R_{4,5} = 2B_{55}, \quad R_{4,7} = 3D_{55}, \quad R_{4,10} = A_{55},$$
$$R_{5,6} = 1, \quad R_{6,3} = 2B_{55}, \quad R_{6,5} = 4D_{55}, \quad R_{6,7} = 6E_{55},$$
$$R_{6,10} = 2B_{55}, \quad R_{7,8} = 1, \quad R_{8,3} = 3D_{55}, \quad R_{8,5} = 6E_{55},$$
$$R_{8,7} = 9F_{55}, \quad R_{8,10} = 3D_{55}, \quad R_{9,10} = 1, \quad R_{10,4} = -A_{55},$$
$$R_{10,6} = -2B_{55}, \quad R_{10,8} = -3D_{55}, \quad R_{10,9} = -\alpha_2, \quad R_{11,12} = 1,$$
$$R_{12,2} = A_{13}, \quad R_{12,11} = A_{33},$$
$$R_{4,12} = B_{55} - B_{13}, \quad R_{6,12} = 2D_{55} - D_{13}, \quad R_{8,12} = 3E_{55} - E_{13},$$
$$R_{12,4} = B_{13} - B_{55}, \quad R_{12,6} = D_{13} - 2D_{55}, \quad R_{12,8} = E_{13} - 3E_{55}.$$

Finally, [T] and λ_i's (i = 1, 2, ..., 12) appearing in Equations (14) are, respectively, the matrix of eigenvectors and eigenvalues of the coefficient matrix [A].